Crystallization of 2-Methyl-1,3-propanediol Substituted Poly(ethylene terephthalate). I. Thermal Behavior and Isothermal Crystallization

Christopher L. Lewis, Joseph E. Spruiell

Materials Science and Engineering, University of Tennessee, Knoxville, Tennessee 37996

Received 6 May 2005; accepted 28 July 2005
DOI 10.1002/app.22786
Published online 2 February 2006 in Wiley InterScience (www.interscience.wiley.com).

ABSTRACT: Differential scanning calorimetry (DSC) was used to evaluate the thermal behavior and isothermal crystallization kinetics of poly(ethylene terephthalate) (PET) copolymers containing 2-methyl-1,3-propanediol as a comonomer unit. The addition of comonomer reduces the melting temperature and decreases the range between the glass transition and melting point. The rate of crystallization is also decreased with the addition of this comonomer. In this case it appears that the more flexible glycol group does not significantly increase crystallization rates by promoting chain folding during crystallization, as has been suggested for some other glycol-modified PET copolyesters. The melting behavior following isothermal crystallization was examined using a Hoffman–Weeks approach, showing very good linearity for all copolymers tested, and predicted an equilibrium melting temperature (T_m^0) of 280.0°C for PET homopolymer, in agreement with literature values. The remaining copolymers showed a marked decrease in T_m^0 with increasing copolymer composition. The results of this study support the claim that these comonomers are excluded from the polymer crystal during growth. © 2006 Wiley Periodicals, Inc. J Appl Polym Sci 100: 2592–2603, 2006

Key words: crystallization; polyester; thermal analysis

INTRODUCTION

Poly(ethylene terephthalate) (PET) is a polymer that has found widespread use and has established itself as arguably one of the most industrially important polyester materials. Many investigators have attempted to improve upon the base PET architecture and properties through copolymerization to produce modified PET copolyesters. As a general rule, adding a comonomer reduces the crystallinity and rate of crystallization. For example, PET copolymerized with the imide containing monomer 4,4′-bis[(4-carbo-2-hydroxyethoxy)phthalimido]diphenylmethane,[1] and polyethylene isophthalate[2] exhibit this effect. It is important to note, however, that many investigators have found evidence suggesting that copolymerizing PET with certain species actually increases the rate of crystallization. Connor et al.[3] found that copolymerizing PET with one of three different comonomers (dimethyl-4–4′-biphenyldicarboxylate, 2,7-dimethyl-4,5,9,10-tetrahydro-pyrenedicarboxylate, or dimethyl-2,7-pyrenedicarboxylate) reduced the overall rate of crystallization. However, it was found that when perylene was added to the copolymers containing pyrene the rate of crystallization was apparently enhanced. It was suggested that this might be due to the formation of π-stacked assemblies of perylene with pyrene, thus forming aggregates that serve as seeds for crystallization. An alternative explanation given was that perylene, upon cooling, first crystallizes, thus acting as a phase-separated, heterogeneous nucleation agent. PET copolymerized with ethylene diamine has also been shown to improve crystallizability.[4] Here, it is speculated that the entropy of crystallization is decreased by the preferential self-assembly of diamide units, facilitated by hydrogen bonding.

Of notable applicability to the present study, Bier et al.[5] found that PET copolymers containing ~5 mol % of branched codiols, such as 2,5-hexanediol and 3-methyl-2,4-pentanediol, crystallized significantly more rapidly than PET homopolymer. In a related study, Bouma et al.[6] found that PET copolymers containing low concentrations of 1,5-pentanediol, 1,8-octanediol, 2,5-hexanediol, or 1,3-dihydroxymethyl benzene were able to enhance nucleation. Bouma et al.[6] found the optimum concentration of 2,5-hexanediol to be 1 mol %, much lower than that suggested by Bier et al.[5] Likewise, it was shown that copolymers containing a branched olefinic diol (C_{36}-diol) were also able to improve crystallizability. Codiols with greater than four carbons are known to fold easily and have a

Correspondence to: J. E. Spruiell (spruiell@utk.edu).
*MPDiol® Glycol is a registered trademark of Lyondell Chemical Company.

lower surface energy than ethanediol.[5–7] As a result, it was speculated that the short codiols, assumed to be rejected from the parent homopolymer crystal but possibly included in the chain fold, enhanced nucleation by decreasing the surface fold free energy. It was further suggested that the inclusion of short methyl groups would decrease the surface free energy to an even greater extent, thus further enhancing this nucleation effect.[6]

A previous study in our laboratory[8] showed that incorporation of small amounts of 2-methyl-1,3-propanediol (referred to hereafter as MPDiol*) into PET had a significant effect on the melt spinability and properties of high-speed spun fibers. The purpose of the present study is to further examine the effect of the incorporation of MPDiol, partially substituted for ethylene glycol on the crystallization behavior of these PET copolyesters. In particular, the thermal behavior and the isothermal crystallization kinetics of samples containing 4, 7, and 10 mol % MPDiol are compared with those of the PET homopolymer.

EXPERIMENTAL

Materials

PET homopolymer and PET copolymers containing MPDiol were supplied by Wellman, Inc. The copolymers were prepared with nominal glycol feed compositions of 4, 7, and 10 mol % MPDiol. Since the reactivity of the polymerizing species in a step polymerizing reaction depend primarily on the reactivity of the functional groups, and not on the actual monomers, it is assumed that the resultant polyesters are random copolymers containing roughly the same composition as in the feed. NMR was used to verify the copolymer composition. This technique gave values of the MPDiol content in these copolymers that was slightly higher than in the feed (5, 9, and 12 mol %). However, the correlation between them was quite good and it was decided to use the nominal composition when reporting the experimental results. The four materials are referred to as PET, PET-4, PET-7, and PET-10, for the homopolymer and the 4, 7, and 10 mol % MPDiol, respectively.

The homopolymer and all three copolymers were supplied in pellet form and had intrinsic viscosities of 0.61 ± 0.01 dL/g.

Sample preparation

All materials were first dried at 100°C in vacuo for at least 12 h prior to sample preparation. Thin films from which the DSC samples were cut were prepared by melt pressing several sliced pellets of each copolymer in a compression molding machine. After cooling from the molding operation, the films were immediately placed in a desiccator until used. DSC samples were cut from the film, using a standard size paper punch and trimmed (if needed) to size.

The isothermal crystallization experiments were carried out in a PerkinElmer DSC7 differential scanning calorimeter, while the thermal characterization of these copolymers was carried out in a Mettler-Toledo DSC820 differential scanning calorimeter. Due to the different types of sample pans for these instruments, the sample sizes for the two types of experiment were slightly different. Samples used in isothermal crystallization experiments were cut to a sample mass of 4.50 ± 0.20 mg, while samples for thermal characterization were cut to 4.00 ± 0.11 mg.

Data collection and analysis

The initial thermal characterization of the materials was performed on melt-quenched samples. This was accomplished by first heating the DSC samples to 290°C in a Mettler FP85 TA cell (equipped with an FP80 central processor). This step was performed not only to heat the sample above its melt temperature for subsequent quenching, but also to destroy any thermal and mechanical history imparted on the sample during melt pressing.

The DSC pans were then quickly submerged in liquid nitrogen and held there for 45 s. An effort was made to ensure that the pan was not tipped or inverted during quenching to guarantee that the melt solidified on the bottom surface of the DSC pan. After quenching, the samples were allowed to stand for no more than 45 min prior to testing, to ensure that annealing effects remained minimal. Samples were then transferred to the Mettler-Toledo DSC820 cell, maintained at 25°C. The DSC was held at 25°C for 5 min to ensure thermal equilibrium was achieved and then heated from 25 to 300°C at a rate of 10°C/min. Three samples of each material were tested in this manner. A pure indium standard, with an onset melting temperature of 156.60°C and a heat of fusion of 28.450 J/g, was used to perform periodic machine calibrations between experimental runs, to ensure data precision.

The isothermal crystallization kinetics were examined using a PerkinElmer DSC7 differential scanning calorimeter, equipped with an FC-50–100-PE intercooler and using a dried nitrogen purge gas. In this experiment, the samples were heated several degrees above their observed melt temperature (T_{hold}) and held at that temperature for 5 min. The hold temperatures used were as follows: PET, 280°C; PET-4, 270°C; PET-7, 270°C; and PET-10, 260°C. This step was performed to erase the mechanical and thermal history of the polymer subjected during sample preparation. The next step was to quench the sample to the isothermal crystallization temperature at a scanning rate of

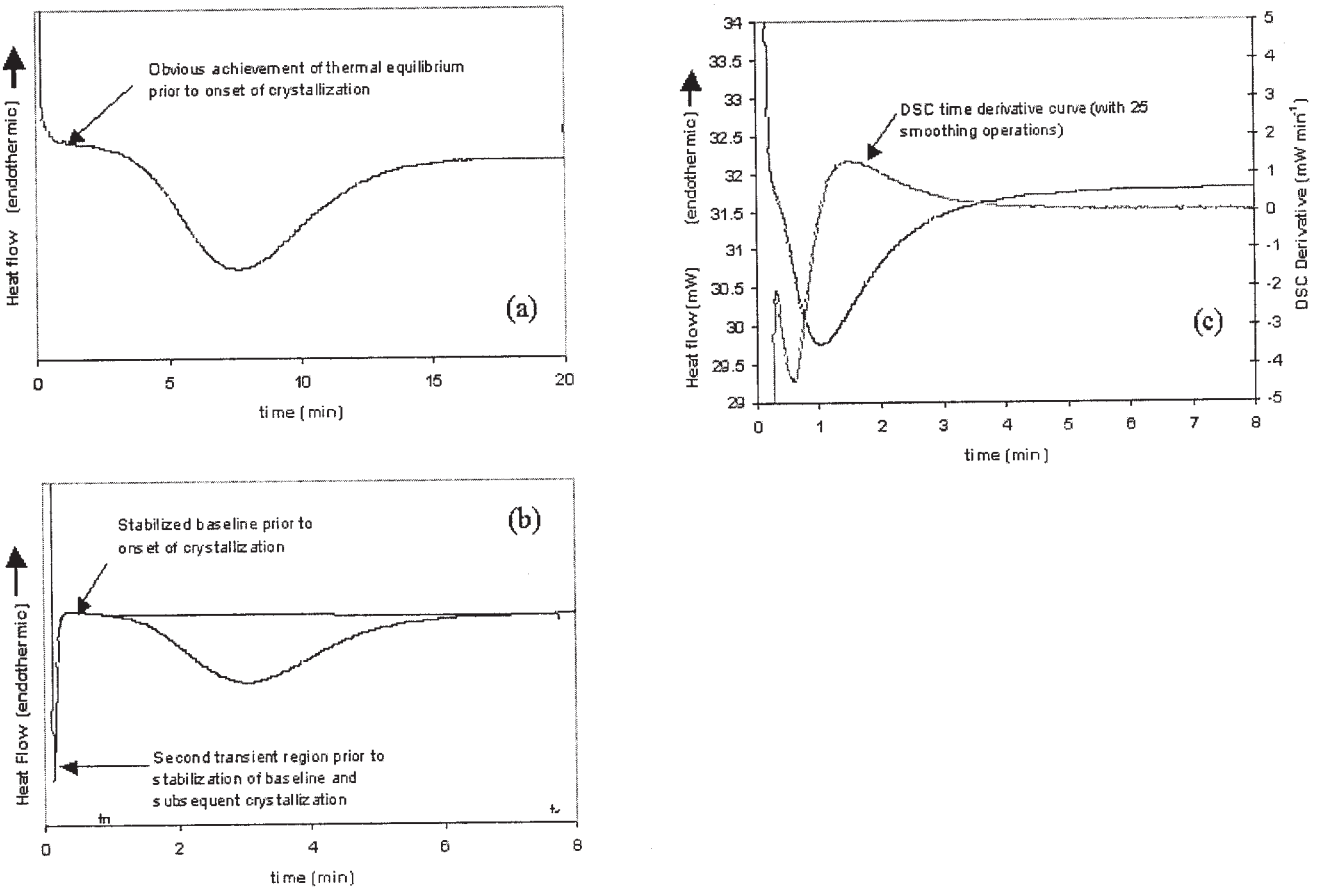

Figure 1 (a) Typical DSC curve encountered at low undercoolings (7 mol % copolyester crystallized at 210°C); (b) exothermic transient response prior to stabilization (4 mol %) copolyester crystallized at 210°C); (c) figure illustrating use of derivative curve to locate t_0.

200°C/min. The sample was allowed to remain at the desired isothermal crystallization temperature until returning to a horizontal baseline, thus indicating the end of crystallization. The samples were then heated at a rate of 25°C/min back to the melt temperature to examine the resulting melting behavior. DSC calibration was performed periodically during testing, using an indium standard to ensure data precision.

The crystallization kinetics was followed by assuming that the relative weight fraction of a crystalline polymer, $\theta(t)$, at time t can be expressed as[9]

$$\theta(t) = \int_0^t (dH/dt)dt \Big/ \int_0^\infty (dH/dt)dt \qquad (1)$$

Therefore $\theta(t)$ can be viewed as a reduced or relative crystallinity, with values ranging between 0 and 1. In practice, the time, t, is determined as the time to reach a particular reduced crystallinity, $\theta(t)$, excluding the time taken to begin the crystallization process, t_0. In this experiment, the induction time was taken as the time of the start of crystallization minus the time where the DSC program first reached the isothermal crystallization temperature, t_T.

During the data collection and analysis, care was taken to ensure that the DSC had reached thermal equilibrium at the crystallization temperature prior to the onset of crystallization in the data reported. Figure 1 shows three types of DSC curves encountered. Figure 1(a) shows the case of low undercooling where the achievement of thermal equilibrium is obvious. Figure 1(b) shows a case exhibiting an exothermal transient prior to baseline stabilization. But the baseline does stabilize sufficiently prior to the onset of crystallization. Figure 1(c) shows the behavior at high undercooling, where the stabilization of the baseline barely occurs prior to the onset of crystallization. In this case, a special derivative technique was used to determine the onset of crystallization; it was taken as the time corresponding to the first peak in the derivative curve. Note that these data were taken using the PerkinElmer DSC, which

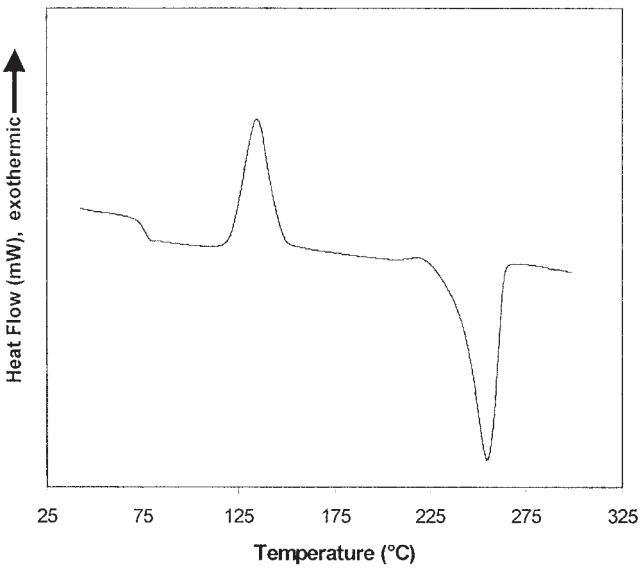

Figure 2 Typical DSC curve for PET homopolymer. Note that the data in this figure were run on the Mettler DSC, which exhibits exothermal peaks above the baseline and endothermal peaks below the baseline.

displays the exothermal peaks (crystallization) in a downward direction.

RESULTS AND DISCUSSION

Thermal characterization

The thermal behavior was investigated using differential scanning calorimetry (DSC) as described earlier. In particular, the glass transition temperature, cold crystallization temperature, and melting peak temperature of samples quenched (from 290°C) in liquid nitrogen were determined.

Figure 2 shows a typical DSC curve observed during this study, in this case for PET homopolymer. These data were run in Mettler DSC, which displays the endothermic transition peaks in a downward direction, while exothermic transition peaks point in an upward direction. Therefore, in this figure the cold crystallization peak points upward and the melting peak points downward.

Glass transition temperature

As would be expected, an increase in the more flexible MPDiol units results in a slight decrease in the glass transition temperature (T_g) (see Table I). Note that all data are reported as the mean of three tested samples plus or minus one standard deviation unless otherwise specified. For PET homopolymer, T_g was determined to be 73.6 ± 1.9°C, which is in good agreement with that reported by others.[10,11] In comparison, the glass transition temperature of the 10 mol % MPDiol material was found to be 69.2 ± 0.4°C, suggesting that the presence of the comonomer units increase the flexibility of the polymer chain. Although the average T_g decreases with increasing comonomer content, it is important to notice that there does not appear to be a significant difference between the glass transition temperatures of the three copolymers tested.

The reduction in the glass transition temperature can be attributed to the following effects: (1) an increase in the length of the flexible group in the main polymer chain (i.e., the presence of an additional methyl group promotes main chain bond rotation); and (2) an increase in free volume associated with the vinyl methyl group (i.e., an increase in the number of flexible side groups).[12] Bond rotation is more easily achieved with increasing number of flexible groups in the main chain of the polymer and therefore less thermal energy is required for molecular motion and rearrangement. The vinyl methyl group acts like an additional chain end and therefore more free volume is achieved at a given temperature. This allows for molecular rearrangements to occur more readily at a given temperature.

Suh et al.[8] found a very similar trend in their analysis of fibers made of PET copolymers containing MPDiol. As with this experiment, it was found that there was a decrease in T_g with increased MPDiol. In their experiments, the glass transition temperatures of PET–MPDiol copolyester fibers spun at low speeds (≈1400 m/min) were determined using DSC. Their results were quite comparable to those found in the present study.

Kiyotsukuri et al.[10] also witnessed similar results when examining the thermal properties of copolymers of PET and 2,2-dialkyl-1,3-propanediols. As with this study, they found only slight changes in the glass transition temperatures for copolymers containing up to 30 mol % comonomer. Likewise, other investigators have found similar decreases in T_g with increasing content of flexible comonomers.[12,6]

Cold crystallization

The cold crystallization behavior of the copolymers reveals that as the concentration of MPDiol is in-

TABLE I
Summary of Glass Transition Data for PET Copolymers

Sample	Mol % Comonomer	Onset Temp. (°C)	T_g (°C)
PET	0	70.3 ± 2.1	73.6 ± 1.9
PET-4	4	67.2 ± 1.6	70.5 ± 1.4
PET-7	7	66.6 ± 1.1	69.8 ± 0.6
PET-10	10	66.8 ± 0.5	69.2 ± 0.4

Limits in all tables based on ±1 standard deviation.

TABLE II
Summary of Cold Crystallization Data of PET Copolymers

Sample	Onset Temp. (°C)	T_∞ (°C)	ΔH_∞ (J/g)
PET	118.6 ± 2.4	129.8 ± 4.2	40.8 ± 0.2
PET-4	120.8 ± 3.3	131.1 ± 3.1	41.8 ± 0.8
PET-7	120.5 ± 0.5	130.6 ± 0.4	40.1 ± 0.5
PET-10	124.3 ± 0.3	135.0 ± 0.5	39.6 ± 0.5

creased there is a slight increase in the cold crystallization temperature (see Table II). This suggests that more thermal energy (and/or time) is required for the molecular rearrangement that is required for nucleation and crystal growth. This has been reported for other PET copolymers as well.[10,1]

What is interesting about these peaks also is the fact that, although they occur at different temperatures, there is no significant difference in the heat released during the exothermic crystallization process for all of the samples tested. Note, however, that the initial crystallinities of the quenched samples were quite different, as described later. This would have a significant effect on the cold crystallization behavior.

Melting behavior

The melting behavior for each of the copolymers tested is given in Table III. Here, it is quite evident that as comonomer content is increased the melt temperature decreases. This can be explained by the notion of comonomer exclusion. As the percentage of comonomer increases, the likelihood of forming lamellae with the same thickness as PET homopolymer decreases. Therefore, as crystal thickness decreases, the surface energy of the crystal becomes more influential, resulting in a depression of the melt temperature. Again, this has been witnessed for many other PET copolymers,[1,13–15] and in particular for those containing short diols.[12,15,16]

Flory's equation[17] for melting point depression was used to examine the melting behavior of these copolyesters. This equation was derived on the assumption that the comonomer units are excluded from the crystals, but they change the configurational entropy of the system, and, therefore, influence the melting temperature. This equation is given by

$$\frac{1}{T_m^0} - \frac{1}{T_m(x_B)} = \frac{R}{\Delta \mathrm{H}_f} \ln(1 - x_B) \qquad (2)$$

where $T_m(x_B)$ is the equilibrium melting temperature of the copolymer with mole fraction of comonomer, T_m^0 is the equilibrium melting temperature of the homopolymer, R is the universal gas constant, and ΔH_f is the heat of fusion.

According to eq. (2), a plot of ${T_m}^{-1}$ as a function of $-\ln(1 - x_B)$ should yield a straight line with y-intercept equal to the reciprocal of the equilibrium melting temperature for PET homopolymer. We have applied this equation to the experimentally measured melting temperatures on the assumption that they are proportional to the equilibrium melting temperatures, as shown in Figure 3. Note that because this equation is applied to the experimentally determined melting temperatures (as opposed to equilibrium melting temperatures) the y-intercept in this particular application should yield an approximate value for the experimentally observed melting temperature of PET homopolymer. This plot was found to show good linearity with an R^2 value of ~1 (see Fig. 3). The intercept in Figure 3 yielded a value for T_m of 251.5°C, close to the experimental value of 253.6°C found for PET homopolymer. The fact that these data appear to fit Flory's equation so well suggests that MPDiol comonomer units are excluded from the parent PET homopolymer crystal.

It should be noted that an effort was maintained to prepare all samples in the exact same manner. It is well established that the initial crystallinity of a sample can be roughly determined by DSC as the difference between the normalized area under the melting endotherm and the cold crystallization peak divided by the heat of fusion of a perfect crystal of that sample. The exact value of the heat of fusion for a perfect PET homopolymer crystal is still somewhat in question, but is reported by Wunderlich[18] as being 140 ± 20 J/g. We used the average value of 140 J/g in this analysis to determine the initial crystallinity of the quenched samples (column 5, Table III). The initial crystallinity of the samples suggests that the crystallization kinetics during the nonisothermal quenching in liquid nitrogen is also affected by increasing comonomer content. PET homopolymer samples showed the highest percent crystallinity (18.0 ± 1.1%), while the 10% MPDiol samples displayed the lowest (8.0 ± 0.3%). The data suggests that the incorporation of MPDiol has an adverse effect on the crystallization kinetics under the moderately high cooling rates associated with quenching in liquid nitrogen.

Suh et al.[8] found somewhat similar results in their study of fiber spinning. In their experiments, it was shown that resins containing 10 mol % MPDiol or less

TABLE III
Summary of Melting Data for PET Copolymers

Sample	Onset Temp. (°C)	T_m (°C)	ΔH_m (J/g)	X_c (%)
PET	238.5 ± 0.6	253.6 ± 0.6	66.1 ± 1.4	18.0 ± 1.1
PET-4	225.8 ± 1.3	243.3 ± 1.1	64.3 ± 4.0	16.1 ± 2.4
PET-7	218.1 ± 0.1	237.4 ± 0.1	56.8 ± 0.5	11.9 ± 0.3
PET-10	212.5 ± 1.6	231.0 ± 0.4	50.8 ± 1.0	8.0 ± 0.3

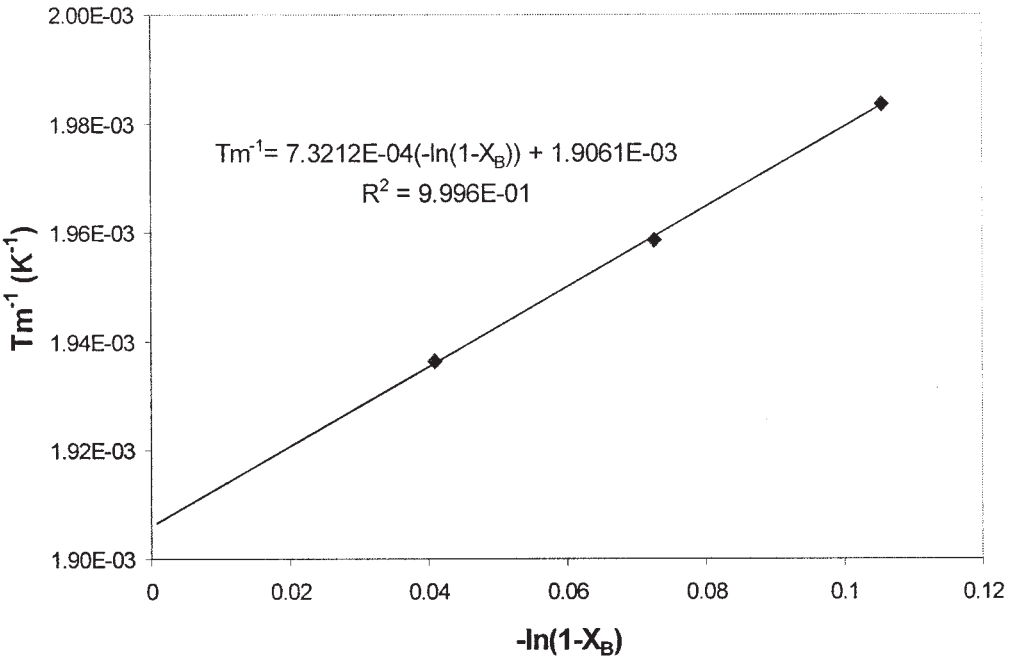

Figure 3 Plot of Flory's equation for PET–MPDiol copolymers.

exhibited appreciable crystallization in the spinline at high spinning speeds, although the presence of MPDiol reduced the crystallinity compared with filaments prepared from PET homopolymer. At the same take-up velocity it was shown that increasing MPDiol content resulted in a decrease in crystallinity, birefringence, and tenacity.

It is well known that the temperature range in which thermal crystallization may occur is defined by the glass transition at the lower limit and the melting temperature as the upper limit. Thus, because the glass transition temperature decreases only slightly with increasing MPDiol content, but the melting temperature decreases significantly, the region within which crystallization is possible decreases with increasing comonomer content. This in itself is a significant result and suggests that the incorporation of MPDiol impedes the crystallizability of these materials and can be used to effectively control the crystallinity of PET.

It should be noted that an additional method of sample preparation was attempted to examine the thermal characteristics of these copolymers, for 100% amorphous starting material. This method involved quenching in ice water. Unfortunately, we were unable to avoid contamination of the quenched samples with water and the results were discarded.

Isothermal crystallization

Relative crystallinity and half-time

Figure 4 shows the relative crystallinity versus time ($t - t_0$) plots for the PET-7 polymer as a function of crystallization temperature. These data show that in the range of temperatures investigated, the crystallization rate decreases with an increase in temperature. Similar behavior was observed for each of the four polymers studied. From these curves the half-time for crystallization was easily determined and these values are summarized in Figure 5, where the half-time of crystallization is plotted as a function of isothermal crystallization temperature. This plot shows that not only does the crystallization half-time increase with increasing crystallization temperature, but also that the crystallization half-time at a given temperature increases with increasing comonomer concentration.

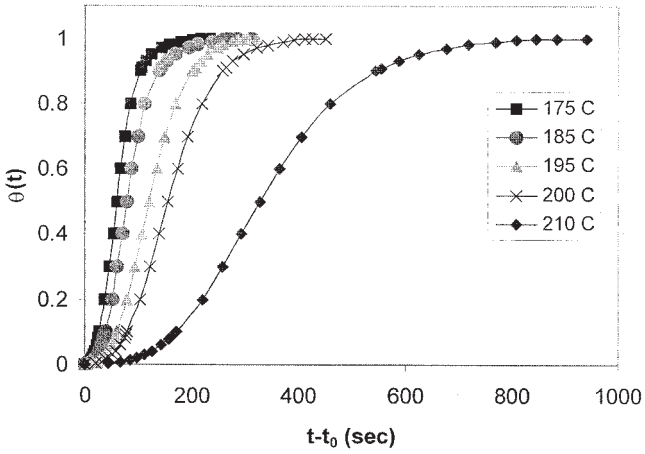

Figure 4 Relative crystallinity versus crystallization time for the PET-7 copolymer.

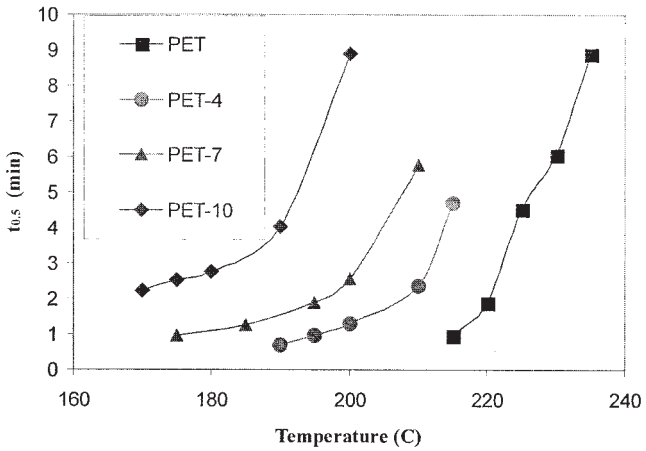

Figure 5 Crystallization half-times of PET and its MPDiol copolymers as a function of isothermal crystallization temperature.

Avrami analysis

The bulk isothermal crystallization kinetics was further examined using the classical Avrami analysis.[19–21] According to the Avrami equation, the relative crystallinity is given by

$$\theta(t) = 1 - \exp(kt^n) \tag{3}$$

where k is Avrami rate constant and n is the Avrami exponent. By this equation a plot of $\ln[-\ln(1 - \theta(t))]$ as a function of $\ln(t - t_0)$ is predicted to yield a straight line with slope equal to n, and y-intercept equal to $\ln(k)$. It is important to note that the Avrami analysis was applied over the range $0.10 \leq \theta(t) \leq 0.80$. It is well known that deviations occur at high values of $\theta(t)$ due to the influence of secondary crystallization processes that are not accounted for in the Avrami analysis.

Avrami plots for the PET-7 copolymer are shown in Figure 6. Similar quality plots were obtained for all of the polymers studied. These plots were used to determine the Avrami exponent, n, and the crystallization rate constant, k. The rate constant can also be determined from the half-time, according to the equation

$$k_{t_{1/2}} = \frac{ln2}{t_{1/2}^m} = \frac{0.693}{t_{1/2}^n} \tag{4}$$

All of the plots of $\ln[-\ln(1 - \theta(t))]$ versus $\ln(t - t_0)$ showed good linearity when performing a linear curve-fit. This was suggested not only by an R^2 value close to 1 (see Table IV), but also when comparing the values of k and $k_{0.5}$ (evaluated using eq. (4)).

Table IV summarizes the results of the isothermal Avrami analysis. As expected, the introduction of MPDiol does reduce the isothermal crystallization rate. The experimental results suggest that under the same operating conditions a 7 mol % copolymer, for example, will crystallize much more slowly, and start crystallizing much later, than PET homopolymer. This is reflected numerically in both the half-time and the value of the rate constant, k. As shown in Table IV, k decreases with increasing copolymer content and with increasing crystallization temperature within the range studied. The rate constants determined using the Avrami analysis and from the half-time using eq. (4) strongly agree.

Note that the values of the Avrami exponents do not exhibit any obvious dependence on either temperature or copolymer content in the range studied; all values were in the range 2.24–3.24 and only one value exceeded 2.77. Such differences are hardly outside the experimental error expected in measurements of the Avrami exponent. This suggests heterogeneous (predetermined) nucleation and three-dimensional growth in these samples, which is consistent with the formation of spherulites or spherulite-like entities.

A possible alternate interpretation that may explain the tendency toward half-integer values of n involves spherical, diffusion-controlled crystallization. For the present PET–MPDiol copolymers, the half-integer values of the Avrami exponent might be explained as being due to a high concentration of noncrystallizable impurities, which must diffuse away from the growth front for crystallization to proceed. For spherical, diffusion-controlled crystallization with thermal (i.e., spontaneous) nucleation,[22] the Avrami exponent approaches a value of approximately 2.5, a value consistent with most of our data. However, a dual mechanism consisting of heterogeneous nucleation with both interface and diffusion controlled growth seems more likely.

Activation energy for crystallization

The activation energy for the overall isothermal crystallization process can be determined by assuming

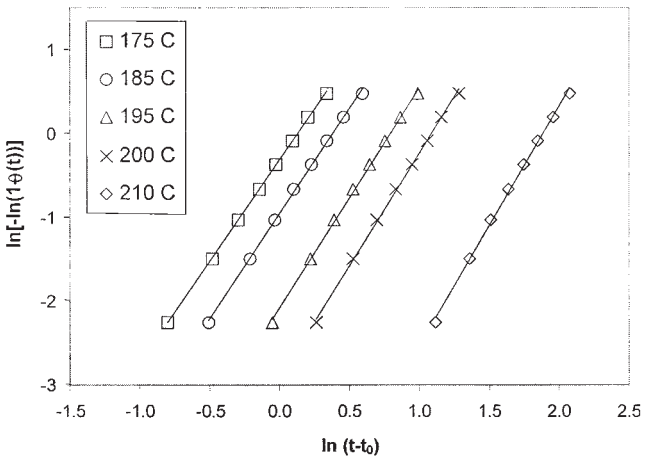

Figure 6 Avrami plots for PET-7 copolymer at different crystallization temperatures.

TABLE IV
Summary of Isothermal Crystallization Kinetics Parameters

Temp. (°C)	t_0 (min)	$t_{0.5} - t_0$ (min)	R^2	n	k (min^{-1})	$k_{0.5}$ (min^{-1})
PET						
215	0.23	0.98	0.996	2.39	0.71	0.722
220	0.41	1.9	0.995	2.62	0.131	0.129
225	0.83	4.57	0.999	2.4	0.017	0.018
230	1.13	6.08	0.998	2.46	0.008	0.008
235	2.63	8.9	0.997	2.24	0.005	0.005
PET-4						
190	0.33	0.71	0.999	2.3	1.48	1.52
195	0.36	0.98	0.999	2.52	0.715	0.728
200	0.44	1.3	0.999	2.68	0.339	0.347
210	0.97	2.38	0.999	2.77	0.061	0.063
215	1.33	4.69	0.998	3.24	0.005	0.005
PET-7						
175	0.35	0.98	0.999	2.41	0.724	0.722
185	0.4	1.26	0.999	2.51	0.381	0.388
195	0.65	1.91	0.999	2.62	0.125	0.128
200	0.91	2.57	0.999	2.68	0.054	0.055
210	2.38	5.75	0.998	2.83	0.005	0.005
PET-10						
170	0.42	2.25	0.999	2.33	0.107	0.105
175	0.46	2.53	0.9995	2.36	0.079	0.078
180	0.5	2.75	0.9995	2.52	0.055	0.054
190	0.9	4.03	0.9999	2.46	0.023	0.023
200	2.13	8.89	0.9999	2.57	0.002	0.003

that the Avrami crystallization rate constant can be described by an Arrhenius-type equation:

$$k^{1/n} = k_0 \exp(-\Delta E/RT) \tag{5}$$

where ΔE is the activation energy, R is the gas constant, and k_0 is a temperature-independent factor.[23] Taking logarithms of this equation leads to the following relation:

$$\left(\frac{1}{n}\right)\ln k = \ln(k_0) - (\Delta E/RT) \tag{6}$$

Using eq. (6), a plot of $(1/n)\ln(k)$ as a function of $1/T$ should yield a straight line with slope $= (-\Delta E/R)$ and y-intercept $= \ln(k_0)$. Such a plot is shown in Figure 7.

It is clear that such plots are not strictly linear as judged from the values of R^2 and the location of the trendlines (see further discussion later) and that such an approach gives, at best, a rough approximation of the true activation energy. On the other hand, it is easy to see that the apparent slope decreases as copolymer content increases. A plot of the apparent activation energies, ΔE, for crystallization is given in Figure 8. What is probably most important to note is not the actual values themselves but rather their trend with copolymer content. These results seem to indicate that the activation energy of bulk, isothermal crystallization increases as a function of copolymer composition. This would indicate that increasing comonomer content results in a less kinetically favorable situation. Thus the energy barrier impeding crystallization appears to increase with increasing comonomer composition.

It is, perhaps, worth noting that for most simple chemical reactions the value of the activation energy is positive and thus a higher value of the activation energy represents an increased energy barrier for the formation of a reaction complex. For these simple

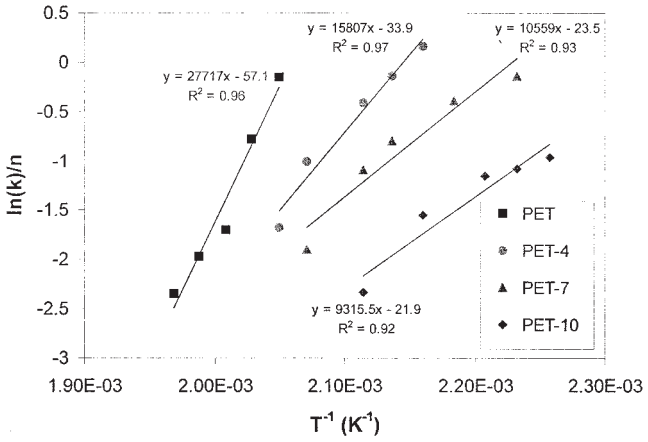

Figure 7 Plot of $\ln(k)/n$ versus reciprocal absolute temperature (data of Table IV).

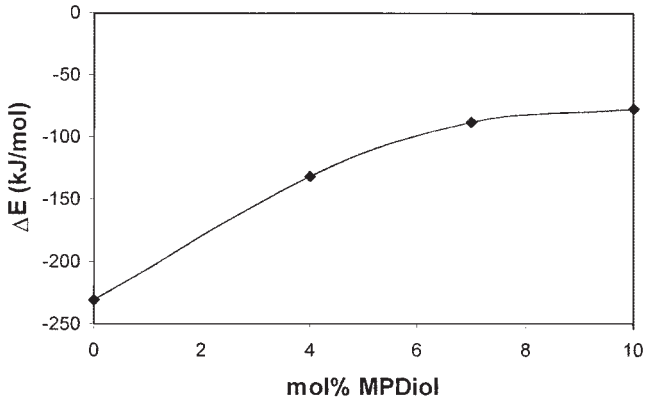

Figure 8 Activation energy for overall crystallization for the present materials.

types of reactions a positive value for the activation energy signifies that the reaction proceeds more rapidly with increasing temperature. This is just the opposite of the case for more complex reactions where reaction rates decrease with increasing temperature. In these cases the sign of the activation energy is negative.[24] This is obviously the case for polymer crystallization in the temperature range investigated, and therefore, by eqs. (5) and (6), a decrease in the value of the activation energy signifies an increase in the rate constant. Thus, because PET has the lowest activation energy, its crystallization is kinetically favored over the copolymers examined.

It should be noted that in their study on the isothermal and cold crystallization kinetics of syndiotactic polypropylenes, Supaphol and Spruiell[25] evaluated the Arrhenius temperature dependence in describing the temperature dependence of the Avrami rate constant. In their study it was shown that, over a wider range of temperatures, the dependence of the Avrami rate constant as a function of temperature resembled the same general shape as a plot of $t_{0.5}$ as a function of temperature, and therefore was anything but linear. This same apparent curvature in the data is found in the data in this experiment, particularly for the copolymer samples, as can be seen by examination of Figure 7. As is explained by Supaphol and Spruiell, this nonlinear dependence should be expected, since the Avrami rate constant is known to be related to the half-time by eq. (4). As is suggested by these authors, over a small temperature range the apparent linearity in the data might lead to a false evaluation of the activation energy. Nevertheless, this analysis has been included because of its widespread use and common acceptance in the literature, and because it does appear to provide for a reasonable way to compare the relative activation energies of these materials in a semiquantitative fashion.

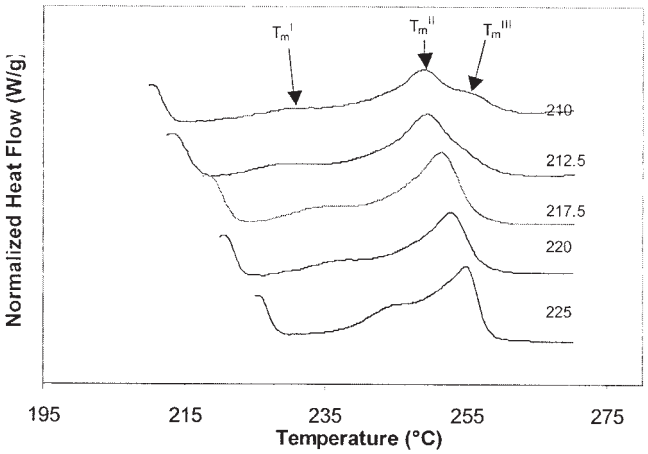

Figure 9 Representative DSC melting curves following isothermal crystallization at the specified temperatures for PET homopolymer. Note that endothermic (melting) peaks point up.

Melting behavior

Upon completion of isothermal crystallization, the samples were immediately reheated to 280°C at a scan rate of 25°C/min, to observe the melting behavior. It is commonly found that PET homopolymer, over a given range of isothermal crystallization temperatures, will often exhibit a multiple peak melting behavior upon subsequent reheating from the isothermal crystallization temperature. In the present study we found that at the lower isothermal crystallization temperatures each of the three copolymers exhibited the multiple melting peaks commonly witnessed for PET homopolymer, as illustrated in Figures 9 and 10 and Table V.

Based on the results in Table V, the third melting peaks appear not to shift significantly with increasing

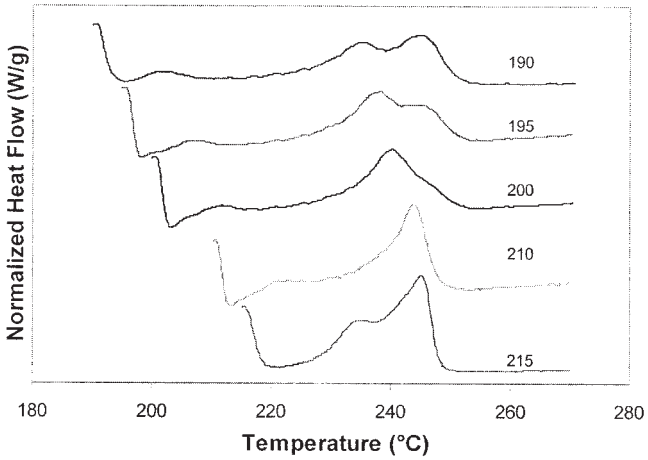

Figure 10 Representative DSC melting curves following isothermal crystallization at the specified temperatures for PET-4 copolymer. Note that endothermic peaks point up.

TABLE V
Summary of Observed Melting Behavior Following Isothermal Crystallization

T_c (°C)	T_m^I (°C)	T_m^{II} (°C)	T_m^{III} (°C)	T_m^0 (°C)
PET				
210	223.1 ± 0.2	248.1 ± 0.4	254.3 ± 0.1	280.0
212.5	229.6 ± 0.3	249.3 ± 0.1	—	
217.5	235.6 ± 0.3	251.4 ± 0.2	—	
220	238.5 ± 0.1	252.6 ± 0.1	—	
225	246.4 ± 0.9	255.0 ± 0.2	—	
PET-4				
190	200.6 ± 0.1	235.0 ± 0.1	244.2 ± 0.4	265.2
195	207.0 ± 0.8	238.5 ± 0.2	246.0 ± 1.3	
200	212.1 ± 0.8	240.3 ± 0.1	—	
210	220.8 ± 0.1	244.1 ± 0.2	—	
215	233.0 ± 1.4	245.0 ± 0.3	—	
PET-7				
175	186.7 ± 0.1	227.3 ± 0.2	238.6 ± 0.1	258.2
185	196.5 ± 0.1	230.5 ± 0.2	238.6 ± 0.1	
195	206.0 ± 0.1	234.5 ± 0.1	—	
200	212.5 ± 0.2	236.7 ± 0.2	—	
210	224.6 ± 0.3	240.1 ± 0.1	—	
PET-10				
170	181.4 ± 0.1	220.6 ± 0.1	232.5 ± 0.1	253.6
175	186.8 ± 0.1	223.1 ± 0.1	232.6 ± 0.1	
180	191.2 ± 0.1	225.1 ± 0.1	232.5 ± 0.1	
190	202.4 ± 0.1	229.2 ± 0.1	—	
200	216.6 ± 0.3	232.4 ± 0.2	—	

crystallization temperature. However, it does appear that the first and second melting peaks both shift to higher temperatures with increasing isothermal crystallization temperature. Additionally, the second melting endotherm appears to increase in magnitude with increasing crystallization temperature at the expense of the third melting peak.

Many investigators attribute the first melting peak to the melting of subsidiary lamellae (from secondary crystallization), the second melting endotherm to the melting of the dominant lamellae, and the third endotherm to recrystallization.[26–28] Thus the equilibrium melting temperature was estimated by the Hoffman–Weeks method,[29] using the peak temperature value of the second melting peak. From Figure 11 it is evident that the Hoffman–Weeks plot showed good linearity. Additionally, the equilibrium melting temperature for PET homopolymer, which was found to be 280.0°C, agreed with that found by other investigators.[30–32]

Although several investigators have used the interpretation described earlier, there is some controversy as to the actual morphological explanation of these three melting endotherms. Medellín-Rodríguez et al.[33,34] recently proposed a somewhat different explanation for the multiple melting endotherms observed in the melting of isothermally crystallized PET samples. In their study, the authors suggested that the first melting endotherm was associated with the melting of the crystals formed during the final stage of secondary crystallization (small branches of metastable crystalline material), the second endotherm was associated with the melting of crystals formed during secondary crystallization (mainly metastable secondary branches), and the third endotherm with the crystals formed during the primary crystallization after having undergone some degree of recrystallization during the heating scan.

Since the physics of this process are still in question, the equilibrium melting point values determined by the Hoffman–Weeks method in this study should be approached with some caution. The values listed in Table V should be viewed as estimates determined with the assumption that the peak melting temperatures of the second melting endotherm are attributed solely to the crystals formed during the isothermal crystallization process. The equilibrium melting point temperatures for the PET copolymers were examined again using the Flory melting point equation (eq. (2)). The Flory equation appeared to fit the experimental data reasonably well ($R^2 = 0.985$), predicting a value of 545.6 K (272.4°C) for the equilibrium melting point of PET homopolymer. Although there is nearly an 8°C difference between this value and the directly measured one, the resulting percent difference between T_m^0 found by the Flory equation and that determined using the Hoffman–Weeks method was found to be 1.38%; this is within the limits of acceptable experimental error considering all sources of error in such measurements.

This experimental piece of evidence appears to further support the claim that MPDiol units are rejected from the parent PET homopolymer crystal, thus resulting in a depression of the melting temperature as the MPDiol content is increased.

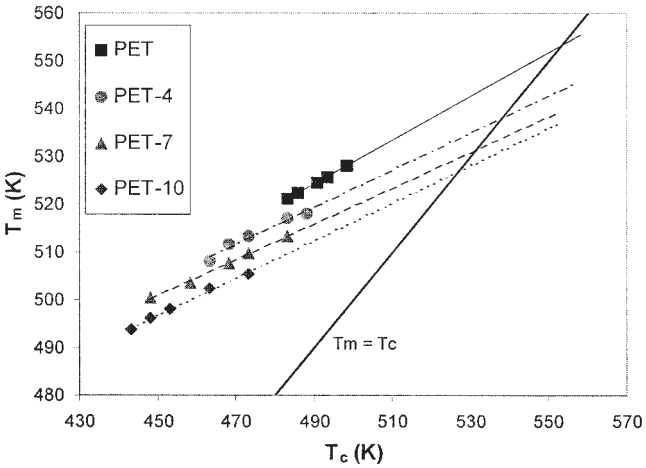

Figure 11 Hoffman–Weeks plot for the four materials.

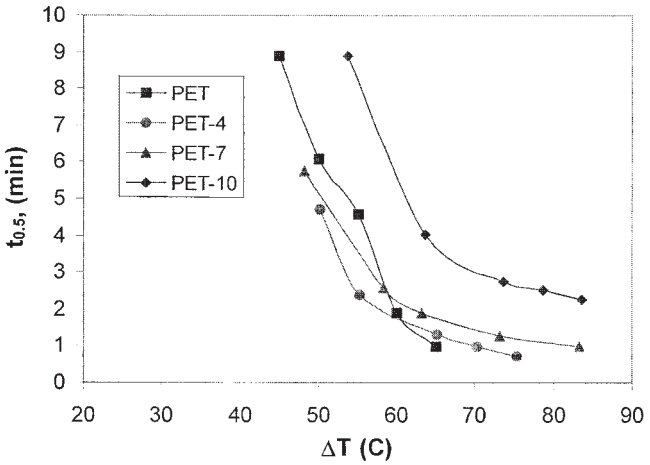

Figure 12 Plot of isothermal crystallization half time as a function of undercooling.

Further discussion of isothermal crystallization results

Determination of the equilibrium melting temperatures for the four materials allows for the isothermal crystallization kinetics to be examined on the basis of the degree of undercooling (i.e., $\Delta T = T_m^0 - T_m$).

A plot of the crystallization half-time as a function of undercooling is shown in Figure 12. Here the data for PET and the 4 and 7 mol % copolymers crystallize at similar rates at a given undercooling. Possibly, the 4 and 7 mol % copolymer crystallize slightly faster than the PET at modest undercoolings.

It would appear that, by this type of examination, copolymer concentrations up to 7 mol % MPDiol appear to slightly enhance crystallization at a given degree of supercooling, at least at modest undercoolings. It is important to note that this does not change the reality that PET crystallizes more rapidly than the other copolymers at a given temperature, but that at modest undercooling, the presence of the comonomer is shown to actually improve the crystallization kinetics with low MPDiol concentration (i.e., $\leq$7 mol %). The 10 mol % copolymer clearly crystallizes at a much slower rate than any of the other materials.

Experimental evidence seems to suggest that the 4 mol % copolymer shows the highest crystallization rate at a given undercooling, at least at modest undercooling. This is in good agreement with reports by others[5,6] who have suggested that PET copolymers containing short codiols exhibit enhanced crystallization rates when comonomer concentration is less than or equal to 5 mol %. This has been explained as being due to increased chain flexibility compared with the more rigid PET molecule, thus allowing for enhanced chain folding during crystallization. However, it appears that too high of a concentration of comonomer negates this kinetically favorable situation because of comonomer exclusion from the parent PET crystal. In the case of MPDiol, it appears that, with regard to undercooling, concentrations less than ~7–8 mol % comonomer appear to show improved crystallizability, with the optimum concentration appearing to be less than or equal to about 4–5 mol % MPDiol.

While the equilibrium melting temperature determined for PET homopolymer in this experiment does agree well with that found by other investigators, the assignment of the melting peaks observed in this experiment are still in question and, as stated earlier, the equilibrium melting temperatures should therefore be approached with some caution.

CONCLUSIONS

1. The melting temperature of PET copolymers containing MPDiol as a comonomer decrease as the content of comonomer increases in good agreement with the Flory theory based on comonomer exclusion from the crystals.
2. The glass transition temperature decreases slightly with the addition of comonomer, but the dependence on concentration is very weak beyond 4 mol % comonomer. Thus, the range between the glass transition and the melting temperature decreases with increase in comonomer concentration.
3. The crystallization rate at a given temperature of these PET copolymers decreases with increase in comonomer concentration. In this case, the more flexible glycol group does not significantly increase the crystallization rates as has been suggested for some other glycol-modified copolyesters.
4. Based on the results of this study, it is concluded that the addition of MPDiol as a comonomer can be used to modify the melting point, crystallization kinetics and, hence, the processing conditions of PET. An earlier study[8] showed that these materials exhibit improved processing during high speed melt spinning of fibers.

The authors thank the Lyondell Chemical Company for their support for the preparation of the polymers used in this study.

References

1. Park, L. S.; Lee, D. C. Polym Eng Sci 1995, 35, 1629.
2. Li, B.; Yu, J.; Lee, S.; Ree, M. Eur Polym J 1999, 35, 1607.
3. Connor, D.; Allen, S.; Collard, D.; Liotta, C.; Schiraldi, D. J Appl Polym Sci 2001, 80, 2696.
4. Bouma, K.; Lohmeijer, J. H. G. M.; de Wit, G.; Gaymans, R. J. Polymer 2000, 41, 3965.
5. Bier, P.; Binsak, R.; Vernaleken, H.; Rempel, D. Angew Makromol Chem 1977, 65, 1.

6. Bouma, K.; Regelink, M.; Gaymans, R. J. J Appl Polym Sci 2001, 80, 2676.
7. Eisenbach, C. D.; Stadler, E.; Enkelmann, V. Macromol Chem Phys 1995, 196, 833.
8. Suh, J.; Spruiell, J. E.; Schwartz, S. A. J Appl Polym Sci 2003, 88, 2589.
9. Vilanova, P.; Ribas, S.; Guzman, G. Polymer 1985, 26, 423.
10. Kiyotsukuri, T.; Masuda, T.; Tsutsumi, N. Polymer 1994, 35, 1274.
11. Ulrich, H. Introduction to Industrial Polymers, 2nd ed.; Hanser: New York, 1993.
12. Ward, I. M.; Hadley, D. W. An Introduction to the Mechanical Properties of Solid Polymers; Wiley: Chichester, 1993.
13. Karayannidis, G. P.; Sideridou, I.; Zamboulis, D.; Bikiaris, D.; Sakalis, A. J Appl Polym Sci 2000, 78, 200.
14. Sakaguchi, Y.; Okamoto, M.; Tanaka, I. Macromolecules 1995, 28, 6155.
15. Sakaguchi, Y. Polymer1997, 38, 2201.
16. Varma, D. S.; Radha, A.; Varma, I. K. Textil Res J 1986, 56, 364.
17. Flory, P. Principles of Polymer Chemistry; Cornell University Press: Ithaca, 1953.
18. Wunderlich, B. Macromolecular Physics, Vol. 3; Academic Press: New York, 1980.
19. Avrami, M. J Chem Phys 1939, 7, 1103.
20. Avrami, M. J Chem Phys 1940, 8, 212.
21. Avrami, M. J Chem Phys 1941, 9, 177.
22. Wunderlich, B. Macromolecular Physics, Vol. 2; Academic Press: New York, 1976.
23. Supaphol, P. J Appl Polym Sci 2000, 78, 338.
24. Atkins, P. W. Physical Chemistry, 4th ed.; W.H. Freeman: New York, 1990.
25. Supaphol, P.; Spruiell, J. E. Polymer 2001, 42, 699.
26. Zhou, C.; Clough, S. B. Polym Eng Sci 1988, 28, 65.
27. Wang, Z.-G.; Hsiao, B. S.; Sauer, B. B.; Kampert, W. G. Polymer 1999, 40, 4615.
28. Lu, X. F.; Hay, J. N. Polymer 2001, 42, 9423.
29. Hoffman, J. D.; Weeks, J. J. J Res Nat Bur Stand Sect A 1962, 66, 13.
30. Miyagi, A.; Wunderlich, B. J Polym Sci Polym Phys Ed 1972, 10, 2085.
31. Taylor, G. W. Polymer 1962, 3, 543.
32. Wlochowicz, A.; Przygocki, W. J Appl Sci 1973, 17, 1197.
33. Medellín-Rodríguez, F. J.; Phillips, P. J.; Lin, J. S.; Campos, R. J Polym Sci Part B: Polym Phys 1997, 35, 1757.
34. Medellín-Rodríguez, F. J.; Phillips, P. J.; Lin, J. S.; Avila-Orta, C. A. J Polym Sci Part B: Polym Phys 1998, 36, 763.